REPORT SD-TR-89-61

(4)

Strong-Inversion Model of Threshold Voltage in Modulation Doped Field-Effect Transistors: The Role of Unintentional Acceptors

R. J. KRANTZ and W. L. BLOSS
Electronics Research Laboratory
Laboratory Operations
The Aerospace Corporation
El Segundo, CA 90245

7 September 1989

Prepared for

SPACE SYSTEMS DIVISION
AIR FORCE SYSTEMS COMMAND
Los Angeles Air Force Base
P.O. Box 92960
Los Angeles, CA 90009-2960

This report was submitted by The Aerospace Corporation, El Segundo, CA 90245, under Contract No. F04701-88-C-0089 with the Space Systems Division, P.O. Box 92960, Los Angeles, CA 90009-2960. It was reviewed and approved for The Aerospace Corporation by M. J. Daugherty, Director, Electronics Research Laboratory.

Lt Jim Emerick was the project officer for the Mission-Oriented Investigation and Experimentation (MOIE) Program.

This report has been reviewed by the Public Affairs Office (PAS) and is releasable to the National Technical Information Service (NTIS). At NTIS, it will be available to the general public, including foreign nationals.

This technical report has been reviewed and is approved for publication. Publication of this report does not constitute Air Force approval of the report's findings or conclusions. It is published only for the exchange and stimulation of ideas.

JIM EMERICK, LT, USAF
MOIE Project Officer
AFSTC/SWL

JAMES A. BERES, LT COL, USAF
MOIE Program Manager
AFSTC/WCO OL-AB

UNCLASSIFIED

SECURITY CLASSIFICATION OF THIS PAGE

REPORT DOCUMENTATION PAGE

1a. REPORT SECURITY CLASSIFICATION Unclassified	1b. RESTRICTIVE MARKINGS
2a. SECURITY CLASSIFICATION AUTHORITY	3. DISTRIBUTION/AVAILABILITY OF REPORT Approved for public release; distribution unlimited.
2b. DECLASSIFICATION/DOWNGRADING SCHEDULE	
4. PERFORMING ORGANIZATION REPORT NUMBER(S) TR-0089(4925-07)-2	5. MONITORING ORGANIZATION REPORT NUMBER(S) SD-TR-89-61
6a. NAME OF PERFORMING ORGANIZATION The Aerospace Corporation Laboratory Operations 6b. OFFICE SYMBOL (If applicable)	7a. NAME OF MONITORING ORGANIZATION Space Systems Division
6c. ADDRESS (City, State, and ZIP Code) El Segundo, CA 90245	7b. ADDRESS (City, State, and ZIP Code) Los Angeles Air Force Base Los Angeles, CA 90009-2960
8a. NAME OF FUNDING/SPONSORING ORGANIZATION 8b. OFFICE SYMBOL (If applicable)	9. PROCUREMENT INSTRUMENT IDENTIFICATION NUMBER F04701-88-C-0089
8c. ADDRESS (City, State, and ZIP Code)	10. SOURCE OF FUNDING NUMBERS PROGRAM ELEMENT NO. / PROJECT NO / TASK NO / WORK UNIT ACCESSION NO.

11. TITLE (Include Security Classification)
Strong-Inversion Model of Threshold Voltage in Modulation Doped Field-Effect Transistors: The Role of Unintentional Acceptors

12. PERSONAL AUTHOR(S)
Krantz, Richard J.; Bloss, Walter L.

13a. TYPE OF REPORT	13b. TIME COVERED FROM ____ TO ____	14. DATE OF REPORT (Year, Month, Day)	15. PAGE COUNT
		1989 September 7	21

16. SUPPLEMENTARY NOTATION

17. COSATI CODES		
FIELD	GROUP	SUB-GROUP

18. SUBJECT TERMS (Continue on reverse if necessary and identify by block number)
MODFET
Strong inversion
Threshold voltage

19. ABSTRACT (Continue on reverse if necessary and identify by block number)

A strong-inversion model, in the depletion layer approximation, of the threshold voltage for modulation doped field-effect transistors (MODFETs) has been developed. We show that for a range of unintentional acceptor doping densities from 10^{13} to 10^{15} cm^{-3} in typical molecular beam epitaxy (MBE)-grown structures, threshold voltages may increase by as much as 200 mV. We isolate the contributions of AlGaAs and GaAs to the threshold voltage. We have verified our model by comparing predicted threshold voltages with those measured in typical MBE-grown MODFET structures.

20. DISTRIBUTION/AVAILABILITY OF ABSTRACT	21. ABSTRACT SECURITY CLASSIFICATION
☒ UNCLASSIFIED/UNLIMITED ☐ SAME AS RPT ☐ DTIC USERS	Unclassified
22a. NAME OF RESPONSIBLE INDIVIDUAL	22b. TELEPHONE (Include Area Code) / 22c. OFFICE SYMBOL

DD FORM 1473, 84 MAR 83 APR edition may be used until exhausted. All other editions are obsolete

SECURITY CLASSIFICATION OF THIS PAGE
UNCLASSIFIED

PREFACE

The authors thank M. J. O'Loughlin, B. K. Janousek, and W. E. Yamada for their invaluable assistance.

CONTENTS

FIGURES

I. INTRODUCTION

Since the original charge-control model for the I-V characteristics of modulation doped field-effect transistors (MODFETs) was developed,[1] a number of models have been proposed.[2-11] In most of these models the density of unintentional acceptor doping, which results as a by-product of the molecular beam epitaxy (MBE) growth process, is ignored when one calculates the electrical characteristics of the device. None of the models includes a precise description of the threshold voltage in MODFET structures; rather, the models all cite V_{off},[1] which is usually considered to be independent of unintentional acceptor doping, as an estimate of the threshold voltage.

In the discussion that follows, we show (1) that the threshold voltage may be defined in the strong-inversion, depletion layer approximation, and (2) that the density of unintentional acceptor doping plays an important role in determining this voltage.

II. STRONG-INVERSION MODEL

The band structure of a typical AlGaAs(n)/GaAs heterojunction with a Schottky barrier at the gate and a spacer layer at the interface under bias is shown in Fig. 1. In most charge-control models, the AlGaAs layer is assumed to be totally depleted during operation[1-3,7,9,10,11] and unintentional acceptor doping in both the AlGaAs and the GaAs layer is ignored. Even in the more complicated descriptions, in which the incomplete ionization of the AlGaAs is included, unintentional acceptor doping is usually ignored altogether[4,5,7,8] or is included only in the GaAs layer.[6] First, we will concern ourselves with the net doping density in each of the regions of the band structure shown in Fig. 1.

A. CHARGE DENSITIES AT THRESHOLD

In the following discussion we assume that all the unintentional acceptors N_a and all the AlGaAs donors are ionized. In the doped AlGaAs layer the charge density is given by

$$\rho_d = q(N_d - N_a) \tag{1}$$

where q is the elemental charge, N_d is the donor concentration in the doped AlGaAs layer, and N_a is the unintentional acceptor doping density throughout the structure.

In the spacer layer a, the charge density is due to the unintentional acceptor doping density; i.e.,

$$\rho_a = -qN_a \tag{2}$$

The region from the interface (d + a) to the edge of the depletion layer (W + d + a) has the following charge density:

$$\rho_W(z) = - q[N_a + n(z)] \tag{3}$$

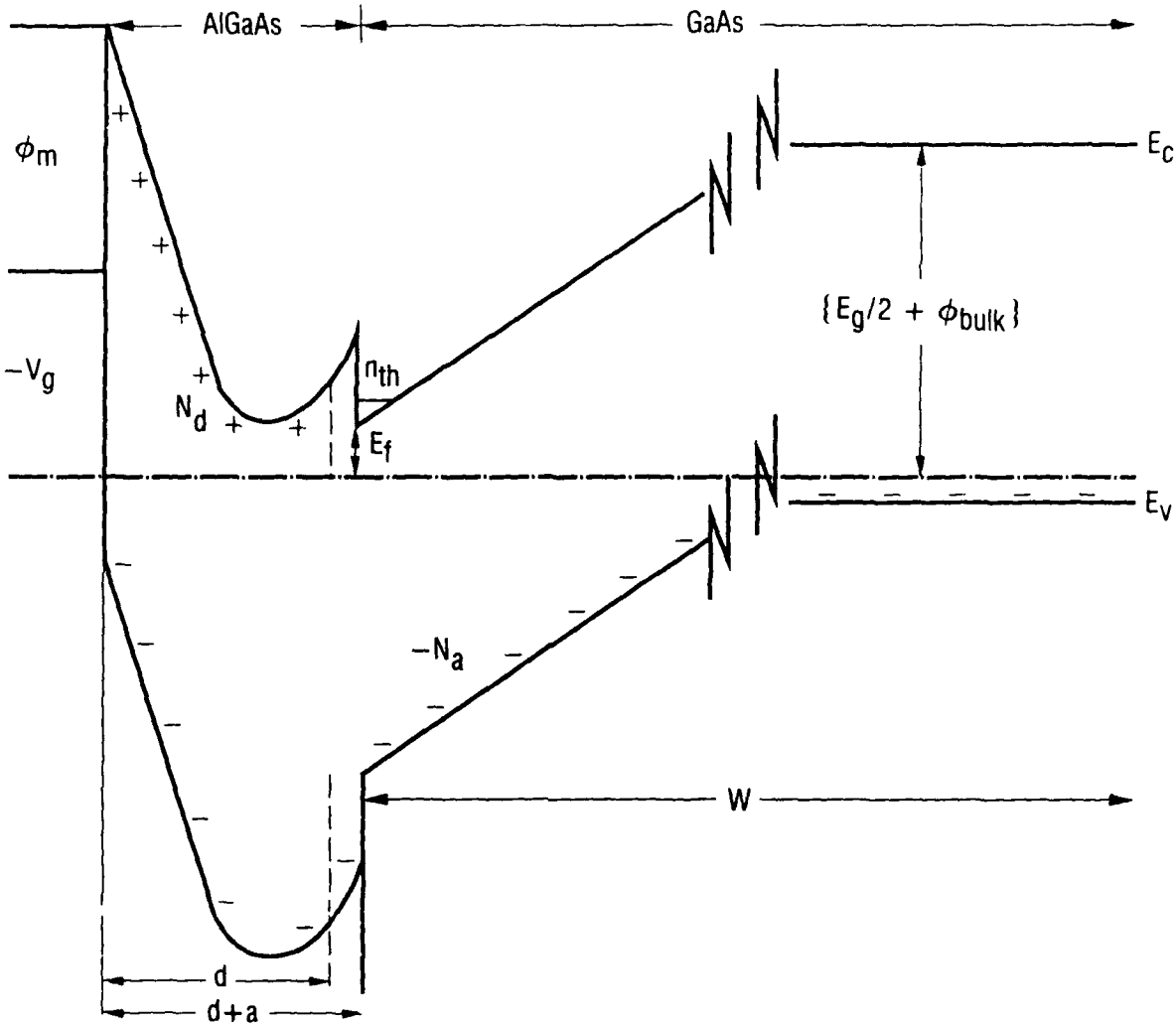

Fig. 1. The Band Diagram of a Typical AlGaAs/GaAs MODFET with Schottky Gate, under Bias V_g, at Threshold. At threshold the AlGaAs donors N_d and unintentional acceptors N_a are assumed to be completely ionized. The charge density in the channel at threshold, n_{th}, is equal to $N_a z_{ave}$ in our strong-inversion model. The Fermi level E_f lies below the bottom of the two-dimensional well at the interface. Band bending from the interface to the edge of the depletion region is the difference between the potential of the conduction band in the bulk, $E_g/2 + \phi_{bulk}$, and the potential at the interface, E_f.

where $n(z)$ is the channel carrier density.

We assume that the channel carrier density at threshold may be written as

$$n(z) = n_{th}\,\delta[z - (d + a + z_{ave})] \tag{4}$$

where n_{th} is the channel carrier density at threshold and z_{ave} is the average position of the channel charge in the two-dimensional (2-D) channel. At threshold we require that the channel carrier density be

$$n_{th} = N_a z_{ave} \tag{5}$$

Therefore, the charge density in the GaAs layer is

$$\rho_W(z) = -qN_a\,\{1 + z_{ave}\,\delta[z - (d + a + z_{ave})]\} \tag{6}$$

Equation (5), for the channel carrier density at threshold, is consistent with the strong-inversion definition of threshold in MOSFETs, where strong inversion occurs when the density of electrons in the channel is equal to the density of acceptors in the bulk. Our definition of strong inversion in MODFETs is the 2-D analog of strong inversion in MOSFETs.

B. THRESHOLD VOLTAGE

The potential V across the structure may be derived in a convenient form by solving Poisson's equation in the following way:

$$V(z) = V_a(z) + V_b(z) \tag{7}$$

where $V_a(z)$ is the solution to the homogeneous equation and $V_b(z)$ is the solution to the inhomogeneous equation with homogeneous boundary conditions. The homogeneous equation yields

$$V_a(z) = -(V_1 - V_2)(z - z_1)/(z_2 - z_1) + V_1 \tag{8}$$

where V_1 is the potential at z_1 and V_2 is the potential at z_2. The inhomogeneous equation may be solved to yield

$$V_b(z) = -[1/\epsilon(z_2 - z_1)][(z - z_2)\int_{z_1}^{z}(z' - z_1)\rho(z')dz' + (z - z_1)\int_{z}^{z_2}(z' - z_2)\rho(z')dz'] \tag{9}$$

where ϵ is the permittivity. Therefore, the potential at any point z in the structure may be written as

$$V(z) = V_1 - (V_1 - V_2)[z - z_1)/(z_2 - z_1)] - [1/\epsilon(z_2 - z_1)][(z - z_2)\int_{z_1}^{z}(z' - z_1)\rho(z')dz' + (z - z_1)\int_{z}^{z_2}(z' - z_2)\rho(z')dz'] \tag{10}$$

We can obtain the field E at any position z by differentiating Eq. (10):

$$E(z) = (V_1 - V_2)/(z_2 - z_1) + [1/\epsilon(z_2 - z_1)][\int_{z_1}^{z}(z' - z_1)\rho(z')dz' + \int_{z}^{z_2}(z' - z_2)\rho(z')dz'] \tag{11}$$

Evaluating Eq. (11) from the gate to the interface and solving for the potential at the gate yields

$$V_G = z_i E_i + V_{i-} - (1/\epsilon)\int_{0}^{z_i}\rho(z')z'dz' \tag{12}$$

where V_G is the potential at the gate and E_i is the field at the interface. Evaluating Eq. (11) from the interface (d + a) to the edge of the depletion layer (W + d + a) and solving for the potential at the edge of the depletion layer yields

$$V_W = -WE_i + V_{i+} + (1/\varepsilon) \int_{z_i}^{W+z_i} (z' - z_2)\rho(z')dz' \qquad (13)$$

where V_W is the potential at the edge of the depletion layer relative to the Fermi level. Subtracting Eq. (13) from Eq. (12) and solving for the potential at the gate yields

$$V_G = (W + z_i)E_i + (V_{i-} - V_{i+}) + V_W - (1/\varepsilon)$$

$$\{\int_0^{z_i} \rho(z')z'dz' + \int_z^{W+z_i} [z' - (W + z_i)]\rho(z')dz'\} \qquad (14)$$

which upon evaluation of the last term may be simplified to yield

$$V_G = (V_{i-} - V_{i+}) + V_W - (1/\varepsilon) \int_0^{W+z_i} \rho(z')z'dz' \qquad (15)$$

where $(V_{i+} - V_{i-})$ is the conduction band offset, and z_i is equal to the sum of the doped AlGaAs layer and the spacer layer, (d + a). The potential at the gate V_G is the difference between the applied potential V_g and the Schottky-barrier height at the gate ϕ_m. Making these substitutions and solving for the applied gate voltage at threshold V_{th} yields

$$V_{th} = \phi_m = \Delta E_c + V_W - (1/\varepsilon) [\int_0^d \rho_d \, z \, dz +$$

$$\int_d^{d+a} \rho_a \, z \, dz + \int_{d+a}^{W+d+a} \rho_W(z) \, z \, dz] \qquad (16)$$

where ΔE_c is the conduction band offset at the AlGaAs/GaAs interface.

In this analysis the dielectric constants of GaAs and AlGaAs are taken to be identical. The potential at the depletion layer edge V_W is the negative of the sum of the potential at the bottom of the conduction band and the band bending from the interface to the depletion layer edge at strong inversion, ϕ_{bb}; i.e.,

$$V_W = -(E_f + \phi_{bb}) \tag{17}$$

In the depletion layer approximation ϕ_{bb} may be calculated by integrating over the charge density from the depletion layer edge to the interface:

$$\phi_{bb} = -(1/\epsilon) \int_{W+d+a}^{d+a} \int_{W+d+a}^{z'} \rho_W(z)dz\, dz' \tag{18}$$

Using Eq. (6) for the charge density in the GaAs region, the band bending from the interface to the edge of the depletion layer is

$$\phi_{bb} = (q/\epsilon)(N_a W^2/2)(1 - 2z_{ave}^2/W^2) \tag{19}$$

Effecting the integrations in Eq. (16), using Eqs. (1), (2), (6), and (19), yields

$$V_{th} = \phi_m - \Delta E_c - E_f + (q/\epsilon)\ \{-(N_d - N_a)d^2/2 +$$

$$N_a W(d + a)\ [1 + \mathcal{O}(z_{ave}/W)]\} \tag{20}$$

for the threshold voltage where terms of order z_{ave}/W will be neglected.

In the typical triangular-well approximation with one subband, the difference between the Fermi energy and the bottom of the 2-D well, at threshold, can be shown to be[1]

$$E_f = -(kT/q)\ln[\exp(\pi\hbar^2 n_{th}/m_1 kT) - 1] - E_0 \tag{21}$$

where k is the Boltzmann constant, T is absolute temperature, h is the Planck constant divided by 2π, m_l is the longitudinal effective mass of the carriers, and E_0 is the energy level of the subband.

At threshold the exponential may be expanded to yield

$$E_f = -(kT/q)\ln(\pi\hbar^2 n_{th}/m_l kT) - E_0 \tag{22}$$

The triangular-well approximation yields the following for the energy of the first subband:

$$E_0 = 9\hbar^2/8m_l)(4E_i m_l/\hbar^2)^{2/3} \tag{23}$$

Integrating the charge density from the interface to the edge of the depletion layer yields the field at the interface:

$$E_i = (q/\varepsilon)\ \{N_a W[1 + \mathcal{O}(z_{ave}/W)]\} \tag{24}$$

where the terms of order z_{ave}/W will be ignored. The triangular-well approximation gives the following for the average channel width:

$$z_{ave} = 3/(4E_i m_l/\hbar^2)^{1/3} \tag{25}$$

The depletion width may be determined from Eq. (19):

$$W = [2(\varepsilon/q)\phi_{bb}/N_a]^{1/2} \tag{26}$$

The band bending ϕ_{bb} may be written in terms of the GaAs band gap, the bulk potential ϕ_{bulk}, and the Fermi potential (see Fig. 1):

$$\phi_{bb} = E_g/2 + \phi_{bulk} - E_f \tag{27}$$

where E_g is the band gap of GaAs and ϕ_{bulk} is the bulk potential in the GaAs. The bulk potential can be calculated by invoking charge neutrality in the bulk. For a p-type material of acceptor density N_a, this yields

$$\phi_{bulk} = (kT/q)\ln(N_A/n_i) \tag{28}$$

where n_i is the intrinsic carrier density of GaAs ($\approx 1.79 \times 10^6$ cm^{-3} at room temperature).

Equation (27) for band bending in MODFETs differs from that in MOSFETs in which the band bending is twice the bulk potential. This difference is due to the 2-D nature of the MODFET structure. To compare the band bending in these two structures, we can write Eq. (27) in the following form:

$$\phi_{bb} = 2\phi_{bulk}[1 + (E_g/2 - \phi_{bulk} - E_f)/2\phi_{bulk})] \tag{29}$$

For high acceptor concentrations ($\approx 10^{17}$ cm^{-3}) the MODFET band bending exceeds the MOSFET band bending by less than 5%, whereas at low acceptor densities ($\approx 10^{13}$ cm^{-3}) the MODFET band bending is almost 40% greater. This difference is reflected in the depletion layer width W. At high acceptor concentrations the MODFET depletion layer is only about 2% larger than the MOSFET depletion layer for the same doping densities. However, at low acceptor concentrations the width of the MODFET depletion layer exceeds that of the MOSFET depletion layer by ≈18%.

The substitution of Eqs. (22) through (28) into Eq. (20) yields a threshold voltage that is a function of the geometric parameters d and a, the donor density N_d, and the unintentional acceptor doping density N_a.

III. THRESHOLD VOLTAGE VERSUS ACCEPTOR DENSITY

In Fig. 2 we show the threshold voltage versus the unintentional acceptor concentration N_a for an AlGaAs doping density N_d of 1×10^{18} cm^{-3} for the structure shown in Fig. 1. The doped AlGaAs layer d is 400 Å wide, the spacer layer a is 30 Å wide, and the GaAs layer is assumed to be semi-infinite. We have isolated the relevant terms in Eq. (20) in order to compare the contributions of each.

At low acceptor densities the threshold voltage is dominated by a combination of (1) the constant term due to the difference between the Schottky-barrier height and the conduction band offset ($\phi_m - \Delta E_c$); (2) the contribution of channel charge to the Fermi energy, $(kT/q)\ln(\pi\hbar^2 n_{th}/m_1 kT)$; and (3) the contribution of doped AlGaAs, $-(N_d - N_a)d^2/2$. The contribution of the first quantum-level energy, E_0, and the contribution proportional to the depletion layer width, $N_a W(d + a)$, are near zero at acceptor densities below $\approx 10^{14}$ cm^{-3}.

As the acceptor density increases, all nonconstant contributions to the threshold voltage increase. Even though the depletion layer width W decreases with increasing acceptor concentration, the depletion layer charge $-qN_aW$ increases, thereby increasing the contribution of the depletion layer to the threshold voltage. As the field at the interface increases as a result of increased charge in the depletion layer, the energy level in the 2-D well also increases as the two-thirds power of the depletion-layer charge, thus also contributing to an increase in the threshold voltage.

Because the channel charge at threshold increases with the acceptor density $N_a z_{ave}$, this contribution also tends to increase the threshold voltage. For all but the highest acceptor concentrations, the contribution of the AlGaAs layer to the threshold voltage is relatively constant; only at acceptor concentrations comparable to the donor density does this term begin to increase appreciably.

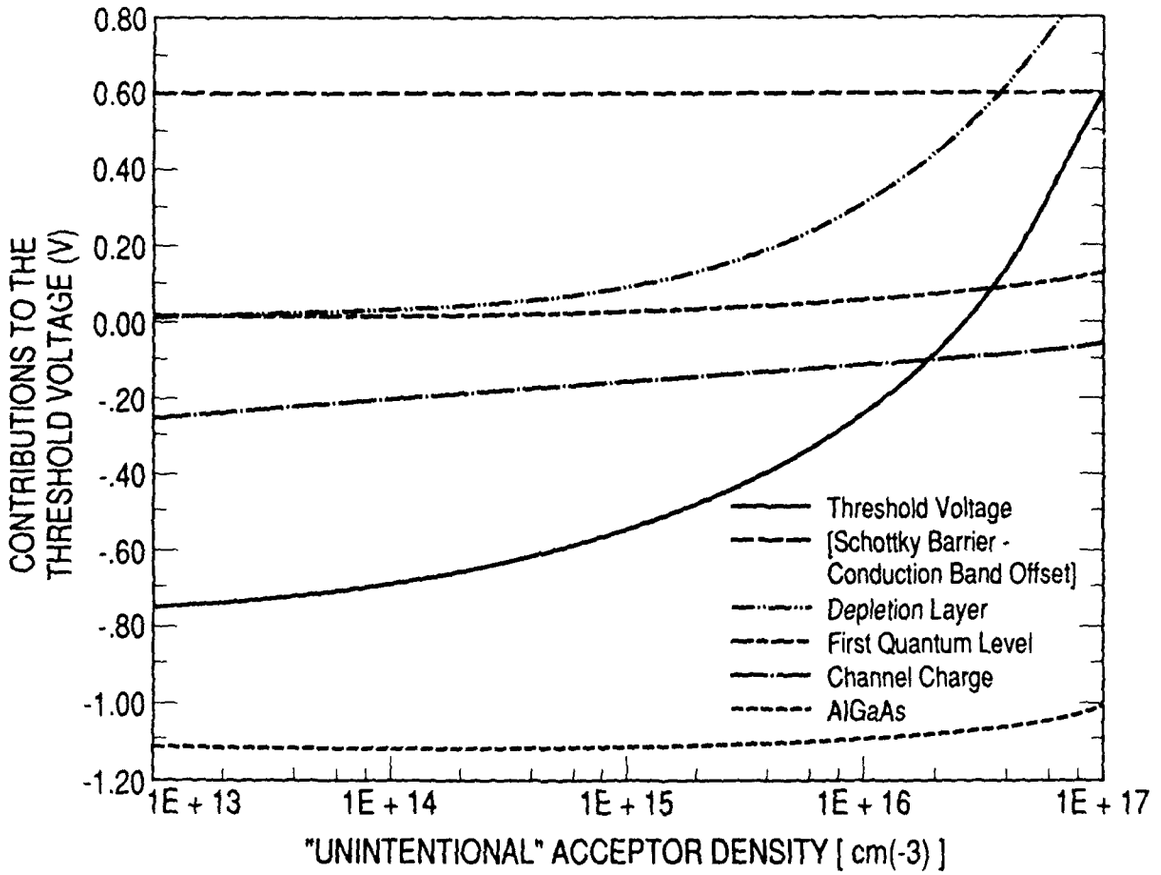

Fig. 2. The Threshold Voltage and Contributions Due to (1) the Height of the Schottky Barrier and the Conduction Band Offset, (2) the Charge of the Depletion Layer, (3) the Position of the First Quantum Level, (4) the Charge Density of the Channel, and (5) the Charge of the AlGaAs Layer versus "Unintentional" Acceptor Doping

As seen in Fig. 2 for unintentional doping densities in the range encountered for typical MBE growth conditions (10^{13} to 10^{15} cm^{-3}), the threshold voltage can increase by as much as 200 mV over this range. At doping densities above this range, the increase in the charge of the depletion layer dominates the increase in the threshold voltage and the threshold voltage rises rapidly.

We have measured the threshold voltage of structures having the geometry cited above with a donor doping density of 1×10^{18} cm^{-3} and an acceptor doping density of 5×10^{14} cm^{-3}. The value of the threshold voltage predicted by our strong-inversion model is -0.620 V (see Fig. 2). This is in reasonable agreement with the measured values, which range from -0.41 to -0.73 V. Variations in the measured values result from variations in the width of the AlGaAs layer that arise from nonuniform processing. The value of the width of the AlGaAs layer, 430 Å, is a nominal value that gives rise to the discrepancy between our calculated value and the measured values.

IV. SUMMARY AND CONCLUSIONS

We have developed a strong-inversion model, in the depletion layer approximation, of the threshold voltage for modulation doped field-effect transistors (MODFETs). The threshold voltage is defined as the voltage at which the channel charge density is equal to the acceptor density times the average channel width. We have experimentally verified the model by comparing predicted threshold voltages with those measured for typical MBE-grown MODFET structures.

We isolate contributions to the threshold voltage that depend on (1) the difference between the height of the Schottky barrier and the offset of the conduction band, (2) the charge of the depletion layer, (3) the energy of the first quantum level, (4) the charge in the 2-D channel, and (5) the density of the AlGaAs donors. At low acceptor densities (below $\approx 10^{15}$ cm^{-3}), the threshold voltage is dominated by the contribution of the AlGaAs layer, the contribution of the channel charge, and the difference between the height of the Schottky barrier and the conduction band offset.

In MODFETs the unintentional acceptor density is usually on the order of 10^{13} to 10^{15} cm^{-3} and the channel width is on the order of 100 Å . Even for these apparently small acceptor densities, especially in comparison with the typical AlGaAs donor densities of $\approx 10^{-18}$ cm^{-3}, we show that the threshold voltage may increase by as much as 200 mV over this range of acceptor densities. Above these acceptor densities the threshold voltage increases rapidly as the charge of the depletion layer increases.

Increasing N_d, the donor density in the AlGaAs layer, would decrease the contribution of AlGaAs to the threshold voltage, thereby offsetting any threshold voltage increase that results from an increase in the unintentional acceptor doping.

The formalism developed in Section II has been applied to the threshold as defined by the strong inversion of the channel. This formalism is by no means restricted to the description of the threshold alone. If one

were to proceed from the equation for the gate potential, Eq. (15), with the assumption that the channel density n_s is much larger than the depletion layer charge $N_a W$, the original charge-control results of Delagebeaudeuf and Linh[1] would be recovered.

REFERENCES

1. D. Delagebeaudeuf and N. T. Linh, "Metal-(n) AlGaAs Two-Dimensional Electron Gas FET," IEEE Trans. Electron Devices ED-29 [6], 955-960 (June 1982).

2. T. J. Drummond, H. Morkoc, K. Lee, and M. Shur, "Model for Modulation-Doped Field-Effect Transistor," IEEE Electron Dev. Lett. EDL-3 [11], 338-341 (November 1982).

3. T. J. Drummond, S. L. Su, W. G. Lyons, R. Fischer, and H. Morkoc, "Design and fabrication of high-transconductance modulation-doped (Al,Ga)As/GaAs FETs," J. Vac. Sci. Technol. B1(2), 186-189 (April - June 1983).

4. K. Lee and M. Shur, "Electron density of the two-dimensional electron gas in modulation-doped layers," J. Appl. Phys. 54(4), 2093-2096 (April 1983).

5. B. Vintner, "Subbands and charge control in a two-dimensional electron gas field-effect transistor," Appl. Phys. Lett. 44(3), 307-309 (1 February 1989).

6. J. Yoshida, "Classical versus Quantum Mechanical Calculation of the Electron Distribution at the n-AlGaAs/GaAs Heterointerface," IEEE Trans. Electron Devices ED-33 [1], 154-156 (January 1986).

7. L. P. Sadwick and K. L. Wang, "A Treatise on the Capacitance-Voltage Relation of High-Electron-Mobility Transistors," IEEE Trans. Electron Devices ED-33 [5], 651-656 (May 1986).

8. S. Subramanian, A. S. Vengurlekar, and A. A. Diwan, "Effect of Shallow and Deep Donors on the Equilibrium Electron Density of the Two-Dimensional Electron Gas in a Modulation-Doped Field-Effect Transistor," IEEE Trans. Electron Devices ED-33 [5], 707-711 (May 1986).

9. A. A. Grinberg, "The effect of the two-dimensional gas degeneracy on the I-V characteristics of the modulation-doped field-effect transistor," J. Appl. Phys. 60(3), 1097-1103 (1 August 1986).

10. Y. M. Kim and P. Roblin, "Two-Dimensional Charge-Control Model for MODFETs," IEEE Trans. Electron Devices ED-33 [11], 1644-1651 (November 1986).

11. W. A. Hughes and C. M. Snowden, "Nonlinear Charge Control in AlGaAs/GaAs Modulation-Doped FETs," IEEE Trans. Electron Devices ED-34 [8], 1617-1625 (August 1987).

LABORATORY OPERATIONS

The Aerospace Corporation functions as an "architect-engineer" for national security projects, specializing in advanced military space systems. Providing research support, the corporation's Laboratory Operations conducts experimental and theoretical investigations that focus on the application of scientific and technical advances to such systems. Vital to the success of these investigations is the technical staff's wide-ranging expertise and its ability to stay current with new developments. This expertise is enhanced by a research program aimed at dealing with the many problems associated with rapidly evolving space systems. Contributing their capabilities to the research effort are these individual laboratories:

Aerophysics Laboratory: Launch vehicle and reentry fluid mechanics, heat transfer and flight dynamics; chemical and electric propulsion, propellant chemistry, chemical dynamics, environmental chemistry, trace detection; spacecraft structural mechanics, contamination, thermal and structural control; high temperature thermomechanics, gas kinetics and radiation; cw and pulsed chemical and excimer laser development including chemical kinetics, spectroscopy, optical resonators, beam control, atmospheric propagation, laser effects and countermeasures.

Chemistry and Physics Laboratory: Atmospheric chemical reactions, atmospheric optics, light scattering, state-specific chemical reactions and radiative signatures of missile plumes, sensor out-of-field-of-view rejection, applied laser spectroscopy, laser chemistry, laser optoelectronics, solar cell physics, battery electrochemistry, space vacuum and radiation effects on materials, lubrication and surface phenomena, thermionic emission, photosensitive materials and detectors, atomic frequency standards, and environmental chemistry.

Computer Science Laboratory: Program verification, program translation, performance-sensitive system design, distributed architectures for spaceborne computers, fault-tolerant computer systems, artificial intelligence, microelectronics applications, communication protocols, and computer security.

Electronics Research Laboratory: Microelectronics, solid-state device physics, compound semiconductors, radiation hardening; electro-optics, quantum electronics, solid-state lasers, optical propagation and communications; microwave semiconductor devices, microwave/millimeter wave measurements, diagnostics and radiometry, microwave/millimeter wave thermionic devices; atomic time and frequency standards; antennas, rf systems, electromagnetic propagation phenomena, space communication systems.

Materials Sciences Laboratory: Development of new materials: metals, alloys, ceramics, polymers and their composites, and new forms of carbon; nondestructive evaluation, component failure analysis and reliability; fracture mechanics and stress corrosion; analysis and evaluation of materials at cryogenic and elevated temperatures as well as in space and enemy-induced environments.

Space Sciences Laboratory: Magnetospheric, auroral and cosmic ray physics, wave-particle interactions, magnetospheric plasma waves; atmospheric and ionospheric physics, density and composition of the upper atmosphere, remote sensing using atmospheric radiation; solar physics, infrared astronomy, infrared signature analysis; effects of solar activity, magnetic storms and nuclear explosions on the earth's atmosphere, ionosphere and magnetosphere; effects of electromagnetic and particulate radiations on space systems; space instrumentation.